Original Article

Evaluation of a novel palatal suture maturation classification as assessed by cone-beam computed tomography imaging of a pre- and postexpansion treatment cohort

Darren Isfeld[a]; Carlos Flores-Mir[b]; Vladimir Leon-Salazar[c,d]; Manuel Lagravère[e]

ABSTRACT

Objectives: To test the reliability and usefulness of the midpalatal suture maturation classification and methodology proposed in 2013 by Angelieri et al. for successful prediction of rapid maxillary expansion (RME) treatment results.

Materials and Methods: Reliability testing focused on 16 patients aged 9.5–17 years with early mixed to full permanent dentition, representing all proposed palatal maturation stages, from available preexpansion cone-beam computed tomography (CBCT). A retrospective observational longitudinal (cohort) study evaluated 63 preadolescent and adolescent patients aged 11–17 years with full permanent dentition treated with tooth-borne RME appliances who had CBCT records taken at pre- (T_1) and postexpansion (T_2). CBCT three-dimensional landmarking produced skeletal and dental widths and dental angulations used to evaluate the extent of skeletal and/or dental expansion. A regression model was used to assess the prediction capability of the T1 palatal suture classification of each subject for dental and skeletal changes.

Results: There was almost perfect intraexaminer agreement and slight to poor interexaminer agreement, differing from previously reported reliability, affected by necessary operator calibration and the degree of postacquisition image sharpness and clarity. Further exploration of its scientific basis suggested that the proposed classification was ill-founded. Results from the cohort study were also wholly unsupportive of efficacy of the proposed palatal suture maturation classification in predicting the magnitude of portrayed changes.

Conclusions: Clinicians should be cautious in applying this classification. Although it has merits, the palatal classification still needs much more research and validation. (*Angle Orthod.* 2019;89:252–261.)

KEY WORDS: Palatal suture; Cone-beam computed tomography; Skeletal maturation

[a] Graduate student, Orthodontic Graduate Program, School of Dentistry, University of Alberta, Edmonton, Alberta, Canada.

[b] Professor and Orthodontic Graduate Program Director, School of Dentistry, University of Alberta, Edmonton, Alberta, Canada.

[c] Clinical Assistant Professor, Division of Pediatric Dentistry, School of Dentistry, University of Minnesota, Minn.

[d] Adjunct Assistant Professor, Orthodontic Graduate Program, School of Dentistry, University of Alberta, Edmonton, Alberta, Canada.

[e] Associate Professor and Orthodontic Graduate Program Director, School of Dentistry, University of Alberta, Edmonton, Alberta, Canada.

Corresponding author: Dr Manuel Lagravère, School of Dentistry, Faculty of Medicine and Dentistry, University of Alberta, ECHA 5-524, 11405 87th Avenue, Edmonton, Alberta T6G 1C9, Canada
(e-mail: manuel@ualberta.ca)

Accepted: September 2018. Submitted: April 2018.
Published Online: November 20, 2018

INTRODUCTION

Literature notes great individual variability in overall skeletal maturation as well as maturation of the midpalatal suture (MPS) and circummaxillary sutures.[1] Fusion of MPS occurs in individuals ranging from 15–19 years old[2] and upward to 71 years,[3] with the greatest degree of sutural obliteration occurring in the third decade of life.[2] As such, these studies suggested that the chronologic age of the patient is an unreliable and poor indicator of the degree of fusion of the maxillary sutures.[4] The variability in the onset of sutural fusion and thus difficulty in predicting the pretreatment degree of MPS maturation creates a unique challenge in treatment planning and delivery of reliable skeletal expansion outcomes in late-stage adolescent and young adult patients.[5] Improper prediction of the pretreatment degree of MPS maturation may lead to

the selection of the least favorable expansion modality being chosen, while putting the patient at higher risk for iatrogenic effects such as acute pain, periodontal recession, mucosal necrosis, severe buccal tipping and associated bite opening, poor transverse and occlusal stability,[5,6] burden of increased cost, pain, healing time, and potentially severe surgical complications.[5] Given that biopsy is the current gold standard to identify the degree of MPS maturation and is unfeasible to be performed on patients, Angelieri et al.[4] developed an imaging protocol and novel, patient-specific classification system dependent upon cone-beam computed tomography (CBCT) imaging of the MPS, assigning an ordinal scale maturation stage (A–E) related to the degree of observed palatal suture fusion. Relating actual pre- and posttreatment clinical rapid maxillary expansion (RME) outcomes and potential cofactors to further evaluate the predictive ability of this novel classification technique is necessary to establish its usefulness to clinical practice and drive RME modality decision making.

With regard to the MPS maturation classification system of Angelieri et al.,[4] the aim of this study was therefore threefold: (1) to determine its reliability, (2) to determine its performance in predicting the success of RME treatment of dental and skeletal changes, and (3) to assess what alteration(s) or modification(s) can be suggested to improve its reliability and/or predictive ability.

MATERIALS AND METHODS

Ethical approval was obtained from the Health Research Ethics Board from the University of Alberta (Pro00060813).

Reliability Testing

Calibration and reliability testing followed the Angelieri et al.[4] protocol. Calibration was performed for all three orthodontic clinicians involved. Although each had a minimum of 3 years of experience in the diagnostic interpretation of CBCT for clinical and/or research purposes, various degrees of comfort with such technology were depicted. Throughout the course of the calibration and reliability testing, evaluations performed by Dr Isfeld were considered the ground truth since this clinician had the most experience with the method itself, as previously defined by Angelieri et al.[4]

The calibration procedure consisted of having Dr Lagravère and Dr Flores-Mir evaluate seven palatal sections separate from the reliability testing sample, representative of maturational stages (A–E), in dimly lit settings without changes to contrast, brightness, or other visual modifications. Drs Lagravère and Flores-Mir were able to openly discuss with each other and Dr Isfeld the appropriate grading of the palatal maturation of these subjects. Any discrepancies or clarification of the stages were open to full discussion and further understanding as needed. Following calibration, Dr Isfeld delivered a second presentation (Microsoft Office PowerPoint 2007, Microsoft, Redmond, Wash) regarding image analysis, detailing the previously developed protocol[4] to isolate palatal axial cross sections from patient three-dimensional (3D) volumes for the purpose of reliability testing.

Reliability testing focused on a total of 16 patients aged 9.5–17 years with early mixed to full permanent dentition who received routine pretreatment CBCTs taken during preliminary record appointments. The CBCT data were generated by an I-CAT machine (120 kVp, 23.87 mAS, 8.9 seconds exposure time, 16- $\times$ 13-cm field of view [FOV], 0.3-mm voxel size). The 16 patients were chosen at random and represented all previously defined[4] maturational stages (A–E). These patients did not have any previous orthodontic treatment, and gender was not taken into account for this part of the study. The three researchers were blinded to all 16 subjects presented during the reliability testing. Reliability testing was performed by having Dr Flores-Mir and Dr Lagravère evaluate the maturational stages of the 16 reliability testing subjects in one viewing session. The clinician representing the ground truth (Dr Isfeld) performed three rounds of evaluations of these patients all 48 hours apart without randomization. All clinicians used the image analysis protocol previously defined[4] to isolate the axial cross sections of the 16 subjects involved in the reliability testing. After isolating the 16 palatal axial cross sections, the clinicians were asked to define the maturational stage in dimly lit settings without changes to contrast, brightness, or other visual modifications.

To conduct the statistical analysis, a standard statistical software package (SPSS version 20 for Mac, IBM, Armonk, NY) was used.

Intraexaminer reliability (Dr Isfeld to Dr Isfeld), interexaminer reliability (Dr Lagravère to Dr Flores-Mir), as well as examiner to ground truth (Dr Lagravère to Dr Isfeld, and Dr Flores-Mir to Dr Isfeld) were investigated by Cohen's Kappa statistic. The kappa statistic results were ascribed according to known guidelines.[7,8]

Predictability Testing

This study evaluated a total of 63 preadolescent and adolescent patients aged 11–17 years with full permanent dentition treated with tooth-borne RME appliances who had CBCT records taken at two time points, T_1 (preexpansion) and T_2 (postexpansion

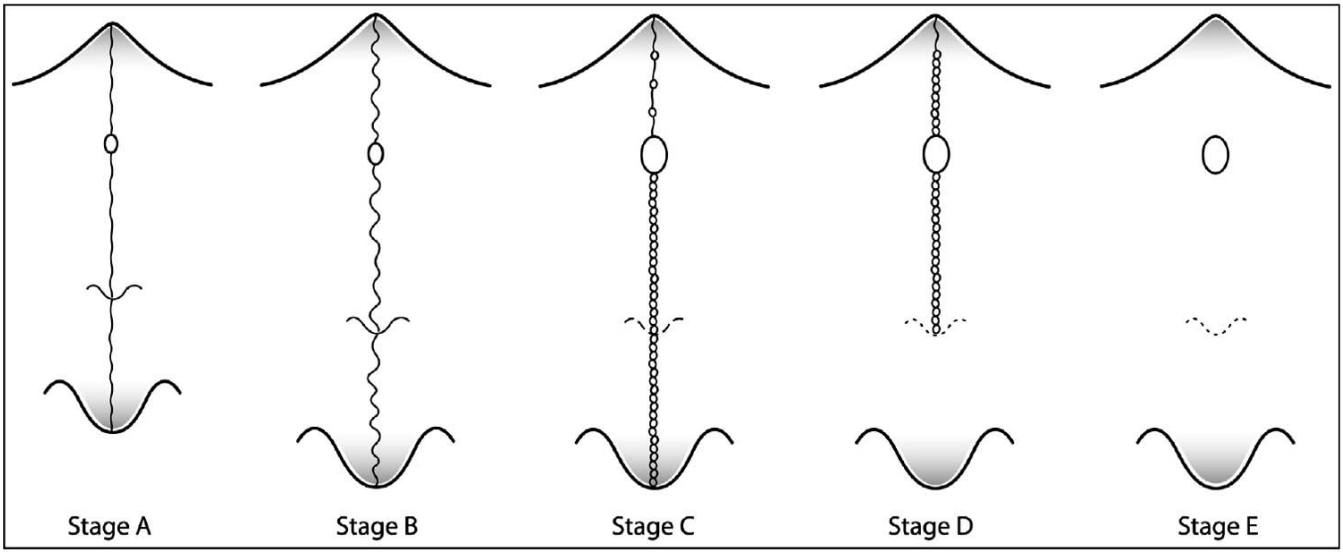

Figure 1. Taken from Angelieri et al.[4] (copyright Elsevier). Diagrammatic representation of the developed novel palate suture maturation classification identifying key radiologic morphologic characteristics specific to each maturity level.

treatment). The image analysis protocol from Angelieri et al.[4] was used to isolate MPS-containing axial cross sections for each patient, to identify the preexpansion sutural maturation stage according to their proposed novel palatal suture maturation classification (Figure 1). In addition, T_1 patient demographics such as age, sex, as well as T_1 cervical vertebrae maturation (CVM) stage were evaluated in the study. The patients were assigned random numbers as patient identifiers.

The investigated CBCT data were derived from a database of patients from a previously published study[9] and another presently ongoing clinical expansion trial. Thus, the sample used for this portion of the study was only the patients who had expansion with the use of a tooth-anchored expander. The CBCT data were generated by an I-CAT machine (120 kVp, 23.87 mAs, 8.9-second exposure time, 16- × 13-cm FOV, 0.3-mm voxel size). Initial pre- and postexpansion CBCT records were gathered using a standardized I-CAT protocol. Captured raw data were exported as DICOM files into Avizo version 7.0 software (Visualization Sciences Group, Burlington, Mass) for further image processing. The software integrated a Cartesian plane coordinate system with various planes, namely, the x-y, x-z, and y-z planes, representing the axial (right-left), coronal (superior-inferior), and sagittal (anterior-posterior), respectively (Figure 2).

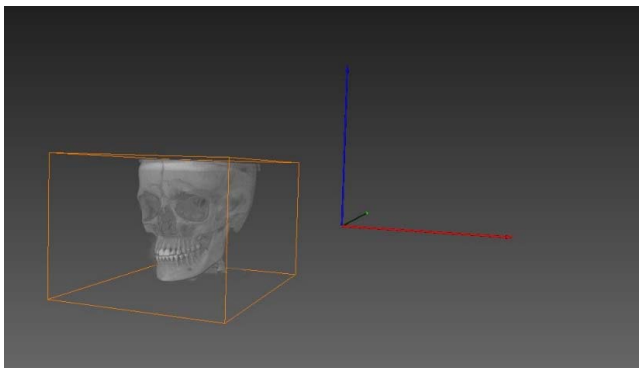

Figure 2. Orientation of the Cartesian plane coordination system in three planes: x (red), y (green), and z (blue).

The Avizo software allowed for 3D landmarking within the Cartesian plane coordinate system, where placement of a landmark was characterized by coordinates in all 3 planes. The primary investigator identified the anatomical locations of interest (Figure 3) and then completed the 3D landmarking by depositing a 0.25-mm-diameter spherical marker within the Cartesian coordinate plane system (Figure 4).

Three-dimensional landmarking in the Cartesian plane coordinate system by a blinded evaluator developed four dental linear measurements, four dental angular measurements, and two skeletal linear measurements (Table 1) to be generated using the equation depicted below:

$$d = \sqrt{(x_2 - x_1)^2 + (y_2 - y_1)^2 + (z_2 - z_1)^2}$$

The distance (d) was measured in millimeters (mm) between the two spherical markers deposited within the coordinate system, and x_1, y_1, z_1 and x_2, y_2, z_2 denoted the coordinates of these landmarks making up the linear measurement. Angular measurements were generated using the following trigonometric equation:

$$a = ACOS(d1*d1 + d3*d3 - d2*d2)/(2*d1*d3)$$

such that $d1$, $d2$, and $d3$ were the distances representing each side of the triangle specific to the

Landmark	Axial View (XY)	Sagittal View (YZ)	Coronal View (XZ)
Pulp chamber (PC)- Upper 1st molar Center of the largest cross sectional pulp chamber area. Defined for both L & R 1st molars: 16 Pulp 26 Pulp	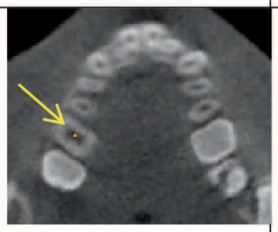		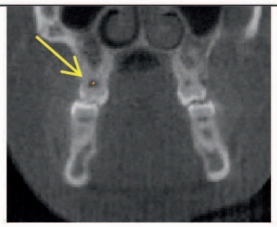
PC- Upper Canines Center of the largest cross sectional pulp chamber area. Defined for both L & R canines: 13 Pulp 23 Pulp	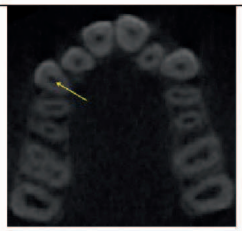		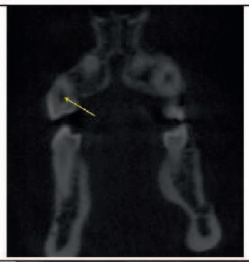
Apex (A) - Upper 1st molar Palatal root apex. Defined for both L & R 1st molars: 16 Apex 26 Apex	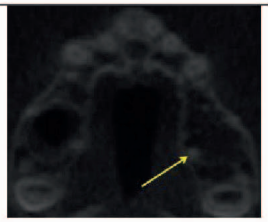		
A - Upper Canines root apex. Defined for both L & R 1st canines: 13 Apex 23 Apex	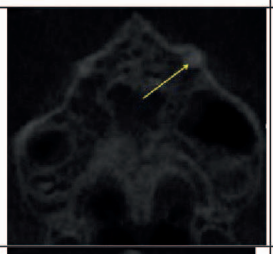		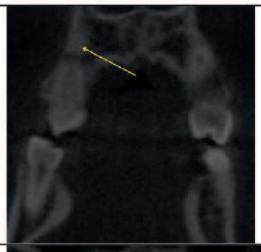
Slope - Point generated at greatest depth of curvature of the palatal slope lingual to the 1st molars. Defined for both L & R slopes.	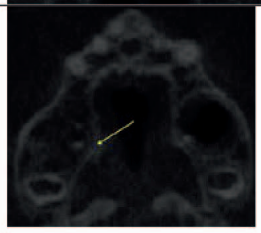	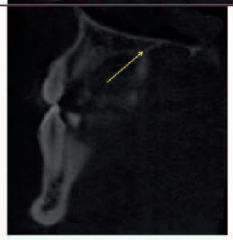	
Infraorbital Foramen (IOF) Superior most aspect of the infraorbital foramen outer border. Defined for both L & R IOF.		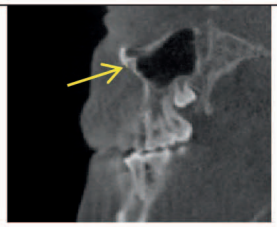	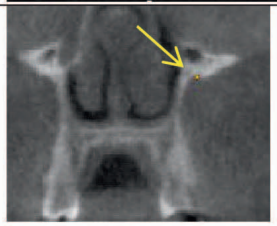

Figure 3. Maxillary landmarks defined and shown on cross-sectional images identified in each subject's pre- and postexpansion CBCT volumes.

Table 1. Dental and Skeletal Linear and Angular Measurements Generated

Dental/ Skeletal	Linear/ Angular	Measurement	Description
Dental	Linear	Intermolar width at the apices	No. 1.6 palatal root apex to No. 2.6 palatal root apex
Dental	Linear	Intermolar width at the pulp chamber	No. 1.6 pulp to No. 2.6 pulp
Dental	Linear	Intercanine width at the apices	No. 1.3 apex to No. 2.3 apex
Dental	Linear	Intercanine width at the pulp chamber	No. 1.3 pulp to No. 2.3 pulp cusp
Dental	Angular	Right canine angulation	No. 1.3 angulation
Dental	Angular	Left canine angulation	No. 2.3 angulation
Dental	Angular	Right molar angulation	No. 16 angulation
Dental	Angular	Left molar angulation	No. 26 angulation
Skeletal	Linear	Inferior orbital foramen (IOF) Distance	R IOF to L IOF
Skeletal	Linear	Palatal width	Palatal alveolar process line of best fit from upper right adjacent to No. 1.6 to upper left adjacent to No. 2.6

location of the angle. The angle (*a*) was defined by radian units and subsequently converted to degrees using Microsoft Excel software (version 15.32, Redmond, Wash). The angle related to the buccal/lingual axial inclination of the tooth in question when viewed in the coronal plane.

The dependent variables, namely, the difference in skeletal and dental distance and dental angles from time 1 (preexpansion) to time 2 (postexpansion; Table 2) were calculated for each subject to evaluate the extent of expansion and infer the type of expansion across the MPS, namely, dentoalveolar and/or skeletal expansion. Consequently, the direction and magnitude of transverse skeletal and dental changes from RME treatment were calculated. If the difference in angular measurements from T1 to T2 were measured to be positive, this related to tooth uprighting, namely, via lingual crown torque and/or buccal root torque from T1 to T2 (Table 3).

Statistical Analysis

The initial statistical analysis was a two-way multivariate analysis of covariance (MANCOVA) considering age and CVM stage as cofactors in relation to the dependent variables. In lieu of any cofactor statistical significance, a multivariate analysis of variance (MANOVA) of the absolute difference between time 1 (T1: preexpansion) and time 2 (T2: postexpansion) was used to determine the significance and test the null hypothesis that a subject's palatal stage has no effect on any of the dependent variables. A *P* value less than .05 was considered significant. An absolute difference $\geq 5^{\circ}$ was considered clinically significant for angular measurements,[10,11] while a difference of equal or greater than 1.0 mm[12] was considered clinically significant for linear measurements.

RESULTS

Reliability Testing

Although there was almost perfect intraexaminer agreement in palatal suture maturation classification by the different investigators, the interrater examiner agreement was only moderate to weak (Table 4). Hence, there was no evidence to support that this level of agreement was greater than solely chance agreement.

Predictability Testing

Upon review, preexpansion palatal staging was unbalanced across the sample (Figure 5a), and therefore, some stages were grouped by reducing the

Table 2. Dependent Variables: Difference in Skeletal and Dental Distances and Dental Angles From T2 to T1

Dental/Skeletal	Linear/Angular	Measurement	Acronym
Dental	Linear	Difference in intermolar width No. 1.6 to No. 2.6 at the apices	Dif_(M_Ap)
Dental	Linear	Difference in intermolar width No. 1.6 to No. 2.6 at the pulp chamber	Dif_(M_Pu)
Dental	Linear	Difference in intercanine width No. 1.3 to No. 2.3 at the apices	Dif_(C_Ap)
Dental	Linear	Difference in intercanine width No. 1.3 to No. 2.3 at the pulp chamber	Dif_C_Pu
Dental	Angular	Change in right canine No. 1.3 angulation	Dif_(ANG_13)
Dental	Angular	Change in left canine No. 2.3 angulation	Dif_(ANG_23)
Dental	Angular	Change in right molar No. 1.6 angulation	Dif_(ANG_16)
Dental	Angular	Change in left molar No. 2.6 angulation	Dif_(ANG_26)
Skeletal	Linear	Change in distance from right to left inferior orbital foramen (IOF)	Dif_(IOF)
Skeletal	Linear	Difference in palatal slope widths	Dif_(slope)

Table 3. Descriptive Statistics of CVM and Repeated Measures for Dental and Skeletal Widths and Dental Angulations

		T1				T2				Difference T2–T1			
Distance	n	Mean at T1	SD	Minimum	Maximum	Mean at T2	SD	Minimum	Maximum	Mean	SD	Minimum	Maximum
CVM	63	3.94	1.18	1	6	—	—	—	—	—	—	—	—
C_Ap	63	23.77	2.81	18.02	29.17	26.83	3.58	19.80	35.86	3.06	2.43	−1.53	8.91
C_Pu	63	29.07	3.10	22.03	36.24	31.15	3.07	21.06	37.42	2.08	2.19	−5.36	8.33
M_Ap	63	30.33	3.43	24.57	39.35	34.17	4.09	25.52	44.18	3.85	2.46	−2.53	8.18
M_Pu	63	40.93	3.22	35.52	49.27	45.68	3.44	38.20	55.23	4.74	2.81	−6.81	11.00
Slope	63	24.85	3.00	15.22	31.67	27.10	3.08	18.79	34.22	2.25	2.11	−7.31	8.19
IOF	63	45.90	3.27	39.13	55.14	47.16	3.36	40.25	54.24	1.26	2.05	−7.10	8.00
ANG_13	63	126.29	9.41	101.66	148.61	132.36	9.32	105.37	153.21	6.07	10.56	−26.37	30.22
ANG_23	63	128.41	11.76	96.86	149.49	135.48	12.64	105.39	158.59	7.06	10.33	−13.28	38.79
ANG_16	63	113.86	8.91	93.50	137.18	116.25	9.97	99.15	147.79	2.39	6.39	−14.39	31.59
ANG_26	63	114.42	10.21	96.75	151.88	117.52	9.77	96.54	153.40	3.10	4.78	−5.99	14.87

number of categories to create balance across the sample to increase the power of the experimental design (Figure 5b).

The new classification grouped the previously defined palatal stages A–E[4] based on the visibility of the MPS in the maxillary and/or palatine bones; stage 1, when MPS was in both palatine and maxillary bone (contains former stages A, B, and C); stage 2, when the MPS was limited to the maxillary bone (formerly stage D); and stage 3, when the MPS was completely fused and nonvisible in either bone (formerly stage E).

The initial statistical analysis used (two-way MANCOVA) revealed that age and CVM stage in relation to the dependent variables were not statistically significant. Consequently, these covariates were not further analyzed.

Thereafter, a one-way MANOVA was performed using palatal stage as the only fixed factor. One-way MANOVA revealed that palatal stage demonstrated convincing statistical significance, $F(20, 102) = 1.709$, $P = .044$; Wilks's $\Lambda = .561$, partial $\eta^2 = .251$.

There was convincing evidence that there was significant difference in Dif_C_Pu and Dif_ANG_16 between subjects with different T1 palatal stages, $F(2, 60) = 3.919$, $P = .025$, partial $\eta^2 = .116$, and $F(2, 60) = 5.588$, $P = .006$, partial $\eta^2 = .157$, respectively. Multiple comparisons of Bonferroni-corrected analyses demonstrated that, at postexpansion, there was a mean increase in intercanine width measured at the pulp in (Dif_C_Pu) between subjects in palatal stage 2 and 3 of 1.7022 mm (95% confidence interval [CI], −0.021 to 3.43), which was suggestive of statistical significance ($P = .054$). In addition, there was a mean increase in the angulation of the right maxillary first molar (Dif_ANG_16) postexpansion between subjects in palatal stage 1 and 3 of 5.635° (95% CI, 1.43 to 9.84), which demonstrated statistical significance ($P = .005$). However, no other group differences were statistically significant.

DISCUSSION

Reliability testing disagreed with that of the original study,[4] indicating that this classification system may not be as reliable as previously presented and that extensive reliability testing is required. This study further revealed that the proposed methodology is in fact nonintuitive, requires major operator calibration, and is heavily influenced by the degree of postacquisition image sharpness and clarity.

There was a clinically significant prediction capability of T1 palatal stage on intercanine width measured at the pulp from stage 2 to stage 3. This was consistent with the inference that expansion occurring during a more immature palatal stage will yield an increasingly efficacious expansion result; however, the mode of expansion, whether it be dentoalveolar, skeletal, or a

Table 4. Intraexaminer, Interexaminer, and Rater to Ground Truth Agreement From Classification of Palatal Suture Maturation (n = 16)[a]

	Kappa	κ	*P* Value
Intraexaminer reliability			
DAI1 vs DAI3	0.915	(95% CI, 0.752 to 1.078)	<.005
ML1 vs ML3	0.903	(95% CI, 0.719 to 1.087)	<.005
CF1 vs CF3	0.911	(95% CI, 0.746 to 1.075)	<.005
ML vs CF	0.040	(95% CI, −0.209 to 0.289)	.733
ML to ground truth (DAI_1)	0.470	(95% CI, 0.141 to 0.799)	.001
CF to ground truth (DAI_1)	−0.015	(95% CI, −0.25 to 0.22)	.896

[a] DAI indicates Dr Isfeld; ML, Dr Lagravère; CF, Dr Flores-Mir.

Table 5. Summary of Histologic Studies Sited as Source of Findings Used to Define the Proposed Palatal Suture Maturational Stages (A–E)[4]

Author	Study Design and Objective	Specimens	Plane of Histologic Sections (Coronal, Sagittal, Axial)
Persson et al. (1978)[13]	Cross-sectional observation study. Objective was to describe the morphology of the initial stages of sutural closure in human and rabbit subjects, to ascertain the role of cellular components during sutural initial stage obliteration process via histochemical and histologic assessment.	**Human material:** Necropsy samples from 24 human subjects aged 15–35 y taken postmortem. Samples are of intermaxillary and transverse palatine sutures of the palate. **Animal material:** Sagittal and interfrontal sutures of rabbits 25–36 mo of age.	Unknown: plane of histologic sections not communicated
Cohen (1993)[15]	Review, to correlate known sutural development and biology to the development of craniosynostosis. Heavy emphasis on review of craniosynostosis-associated literature. Brief review of findings of Persson et al. (1978).[13]	Not applicable	Not applicable
Sun et al. (2004)[14]	Investigated the effect of masticatory strain in the posterior interfrontal and anterior interparietal sutures. In addition, growth was quantified at said sutures and adjacent bone surfaces.	**Animal material:** 14 Hanford miniature pigs (*Sus scrofa*, Charles River Labs); four 3-mo-old, four 5-mo-old, and six 7-mo-old miniature swine.	Coronal plane

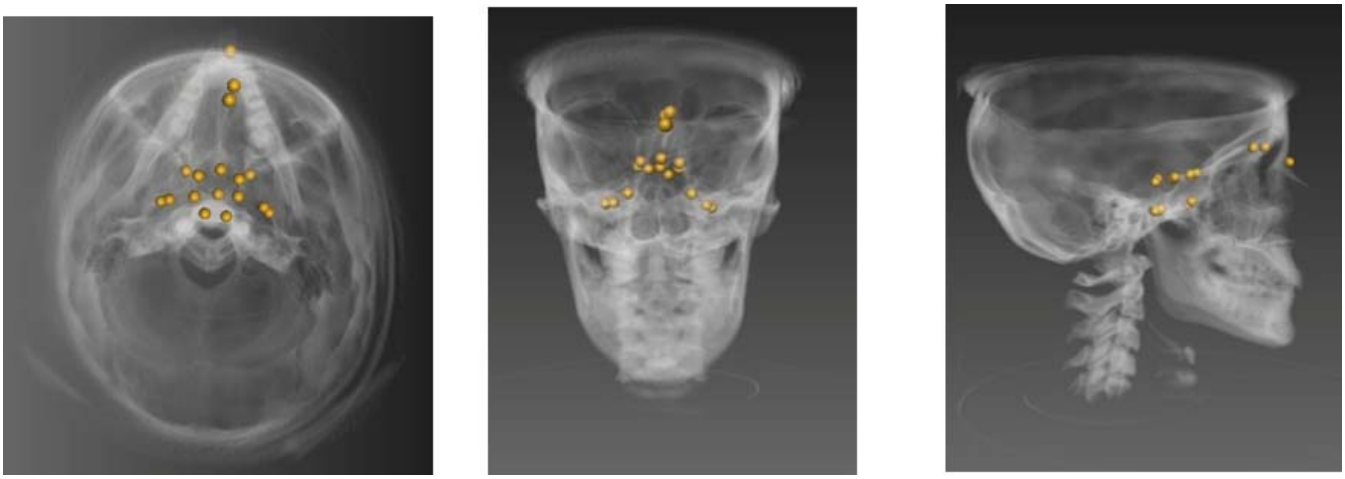

Figure 4. Spherical markers representing the 3D landmarks of interest, visualized in the x, y, and z planes within Avizo software version 7.0.

Table 5. Extended

Characteristics of Histologic Sections	Magnification	Comments
Collagen fiber bundles demonstrate two structural patterns: oriented perpendicular and parallel to sutural margins. Dense bundles of perpendicular fibers were at times observed to be tendon-like. Two patterns of initial obliteration observed: First, presence of one or more bone spicules extending from sutural margins into sutural gap and/or extending to bridge entirety of sutural gap. Spicules tended to be found in more mature specimens. Second (found almost exclusively to human MPS), presence of irregular, heterogeneous, acellular calcified bodies with clearly demarcated margins, existing freely in the sutural gap, or extending from bone spicules from the sutural margins. Multiple bodies may coalesce to form a larger calcified mass. Cystlike spaces may exist. In addition, other specimens with woven bone had to bridge the sutural gap.	All specimens evaluated at 250×	Distribution of female and male samples not given. The plane of the photomicrographs taken for the study also unknown/not communicated. Study found that suture obliteration took place via intramembranous ossification, where transsutural tendonlike tissue is located. There was no radiologic evaluation of the sutures of interest nor radiomorphologic description thereof.
Review reiterated findings of Persson et al. (1978)[13]	Not applicable	Paper was a review and delivered no advanced histologic findings related to the MPS not previously described by Persson et al. (1978).[13] No radiologic evaluation of the MPS or facial sutures nor radiomorphologic description thereof.
Interparietal sutures of all subjects were straight/flat or mildly irregular in morphology, being closed only on the ectocranial aspect and patent (yet narrower) on the endocranial aspect. Interfrontal suture displayed complex internal interdigitation. Interfrontal suture of all 3-mo-old pigs was interdigitated, in the 5- and 7- mo-old pigs the endocranial aspect of this suture was interdigitated, while the ectocranial aspect was relatively straight/flat. Suture width was greater on the ecto- rather than endocranial aspect of the sutures for both the interfrontal and interparietal sutures. In flat areas, Sharpey's fibers were positioned perpendicularly into the bony margins, and in the interdigitated aspects the collagen fibers were positioned obliquely to the bony margins.	Calibration bar at 500 μm and 1000 μm	Findings contradict human suture fusion, which occurs from the endocranial aspect. There was no radiologic evaluation of the sutures of interest nor radiomorphologic description thereof.

combination thereof, remained ambiguous from the current findings.

Results suggested a clinically significant prediction capability of T1 palatal stage on the angulation of the maxillary right first molar (No. 1.6) from palatal stage 1 to 3. However, because of the bilateral nature of any sort of expansion across the suture, a lack of significant findings as it related to the angulation of the contralateral molar (No. 2.6) indicates these results should be taken with caution. In fact, there were eight other dental widths, angles, and skeletal widths that were not meaningfully predicted by the patients' palatal stage at T1. Consequently, it was inferred that palatal stage at T1 truly had little to no prediction capability on these important and clinically relevant angulations and widths during the expansion treatment.

Because of the highly unsupportive results of this study, a review of the basis for the theoretical development of the novel palatal suture classification[4] was performed. The authors of the proposed maturation classification[4] referenced three histologic studies used to develop the basis of the novel classifications (Table 5), and multiple concerns were identified in using these studies to develop the novel classification. The use of specimens of species other than human autopsy material, evaluation of photomicrographs in the coronal plane rather than the axial plane, using an improper age of human specimens that would not include subjects with patent or immature sutures, and correlating the morphology of highly magnified histologic photomicrographs to eye-level CBCT-generated axial cross sections presented great concerns. Consequently, utilization of these studies[13–15] to draw inferences into the radiologic morphology of the MPS in axially generated cross sections is significantly cautioned. As a result, it is advisable that, until further research supportive of this classification[4] is developed and rigorously tested, clinicians do not consider this

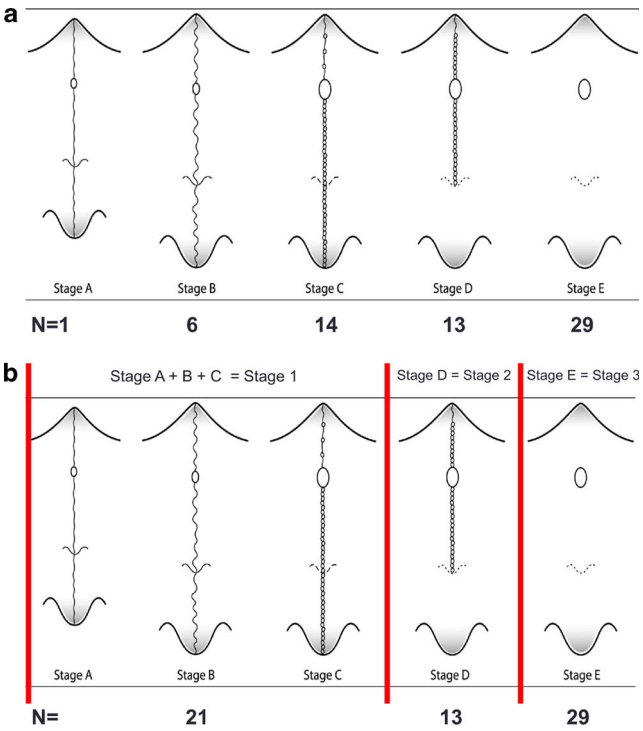

Figure 5. (a) Unbalanced distribution of palatal states across the sample (n = 63) as classified according to Angelieri et al.[4] (b) Improved, balanced distribution of palatal states across the sample (n = 63) after implementation of a modified Angelieri et al.[4] classification.

proposed classification[4] as being factual and should halt employing its use to drive clinical decision making. The findings of this study suggested that improvement of the proposed classification[4] would require a comprehensive overhaul of its scientific basis and would need rigorous testing against a gold standard.

Limitations

Major limitations of this study and the study in question[4] included lack of a gold standard, that being biopsy of the MPS. The proposed classification[4] was based on the qualitative interpretation of the MPS in the axially generated slices which, in itself, was a limitation because of the subjective nature of this interpretation. This was further compounded by the large voxel size, constraining the axial cross-section thickness to a default of 1.0 mm and associated poor image clarity, which negatively affected the visualization and interpretation of the radiomorphology of the T1 MPS, rendering the classification of subjects increasingly difficult. Poor image quality affected both the reliability testing and assessment of the efficacy of the classification to predict the success of RME therapy. These findings were directly attributable to the poor reliability findings (Table 3) and were a significant source of difficulty in staging subjects. Memory bias may have confounded the reliability testing results due to the passage of 48 hours between ranking sessions by the ground truth examiner.

CONCLUSIONS

- Reliability testing disagrees with that of the original study.[4] The proposed methodology is nonintuitive, requires significant operator calibration, and is heavily influenced by the degree of postacquisition image sharpness and clarity.
- Assigned palatal stage at T1 had little to no predictive capability on the dependent variables related to the extent and direction of expansion across the MPS.
- Clinicians should be cautious in applying this classification. Although it has its merits, the palatal classification still needs much more research and validation.

REFERENCES

1. Kosowski TR, Weathers WM, Wolfswinkel EM, Ridgway EB. Cleft palate. *Semin Plast Surg*. 2012;26:164–169.
2. Baccetti T, Franchi L, Cameron CG, McNamara JA Jr. Treatment timing for rapid maxillary expansion. *Angle Orthod*. 2001;71:343–350.
3. Persson M, Thilander B. Palatal suture closure in man from 15 to 35 years of age. *Am J Orthod*. 1977;72:42–52.
4. Angelieri F, Cevidanes LH, Franch L, Gonçalves JR, Benavides E, McNamara JA Jr. Midpalatal suture maturation: classification method for individual assessment before rapid maxillary expansion. *Am J Orthod Dentofacial Orthop*. 2013;144:759–769.
5. Revelo B, Fishman LS. Maturational evaluation of ossification of the midpalatal suture. *Am J Orthod Dentofacial Orthop*. 1994;105:288–292.
6. Melsen B, Melsen F. The postnatal development of the palatomaxillary region studied on human autopsy material. *Am J Orthod*. 1982; 82:329–342.
7. Landis JR, Koch GG. The measurement of observer agreement for categorical data. *Biometrics*. 1977;33:159–174.
8. Viera AJ, Garrett JM. Understanding interobserver agreement: the kappa statistic. *Fam Med*. 2005;37:360–363.
9. Lagravère MO, Major PW, Carey J. Sensitivity analysis for plane orientation in three-dimensional cephalometric analysis based on superimposition of serial cone beam computed tomography images. *Dentomaxillofac Radiol*. 2010;39:400–408.
10. Cao L, Zhang K, Bai D, Jing Y, Tian Y, Guo Y. Effect of maxillary incisor labiolingual inclination and anteroposterior position on smiling profile esthetics. *Angle Orthod*. 2011; 81: 121–129.
11. Chirivella P, Singaraju GS, Mandava P, Reddy VK, Neravati JK, George SA. Comparison of the effect of labiolingual inclination and anteroposterior position of maxillary incisors on esthetic profile in three different facial patterns. *J Orthod Sci*. 2017;6:1–10.

12. O'Higgins EA, Kirschen RH, Lee RT. The influence of maxillary incisor inclination on arch length. *Br J Orthod*. 1999;26:97–102.
13. Persson M, Magnusson BC, Thilander B. Sutural closure in rabbit and man: a morphological and histochemical study. *J Anat*. 1978;125:313–321.
14. Sun Z, Lee E, Herring SW. Cranial sutures and bones: growth and fusion in relation to masticatory strain. *Anat Rec A Discov Mo Cell Evol Biol*. 2004;276:150–161.
15. Cohen MM Jr. Sutural biology and the correlates of craniosynostosis. *Am J Med Genet*. 1993;47:581–616.